Citation: Cell Death and Disease (2011) 2, e122; doi:10.1038/cddis.2011.4

www.nature.com/cddis

Gadd45α activity is the principal effector of *Shigella* mitochondria-dependent epithelial cell death *in vitro* and *ex vivo*

L Lembo-Fazio[1], G Nigro[1,7], G Noël[1], G Rossi[2], F Chiara[3,4], K Tsilingiri[5], M Rescigno[5], A Rasola[3] and ML Bernardini*[,1,6]

Modulation of death is a pathogen strategy to establish residence and promote survival in host cells and tissues. *Shigella* spp. are human pathogens that invade colonic mucosa, where they provoke lesions caused by their ability to manipulate the host cell responses. *Shigella* spp. induce various types of cell death in different cell populations. However, they are equally able to protect host cells from death. Here, we have investigated on the molecular mechanisms and cell effectors governing the balance between survival and death in epithelial cells infected with *Shigella*. To explore these aspects, we have exploited both, the HeLa cell invasion assay and a novel *ex vivo* human colon organ culture model of infection that mimics natural conditions of shigellosis. Our results definitely show that *Shigella* induces a rapid intrinsic apoptosis of infected cells, *via* mitochondrial depolarization and the ensuing caspase-9 activation. Moreover, for the first time we identify the eukaryotic stress-response factor growth arrest and DNA damage 45α as a key player in the induction of the apoptotic process elicited by *Shigella* in epithelial cells, revealing an unexplored role of this molecule in the course of infections sustained by invasive pathogens.
Cell Death and Disease (2011) **2,** e122; doi:10.1038/cddis.2011.4; published online 24 February 2011
Subject Category: Immunity

In the course of a bacterial infection, complex molecular interplays occur between host cells and bacteria. To eradicate or contain the infection, myeloid cells activate strategies aimed at destroying the pathogen, whereas epithelial cells are committed to reduce the bacterial loading. This can be achieved by the suicide of infected cells, mainly through activation of programmed cell death (PCD) or of the autophagic process.[1] Conversely, pathogens deal with the need to establish a replicative niche in the host and to assure their own survival. This can be obtained by inducing apoptosis or pyroptosis in the host cell;[1] however, bacteria can also protect the infected cells from PCD or provoke necrosis or, finally, interfere with the autophagic process.[2] Notably, the possibility exists that these mechanisms are not mutually exclusive, and that the choice among them depends on several factors, including the kinetics and route of infection, the cell population infected, and on the specific pathogen.

This complexity of regulatory mechanisms is observed in the invasive process of *Shigella* spp., an enteric pathogen that causes bacillary dysentery in humans.[3] The pathogenicity of *Shigella* resides on the ability to invade the colonic mucosa through secreted effectors that allow these bacteria to penetrate epithelial cells, to escape from the phagocytic vacuole and to disseminate throughout the epithelium.[4,5]

In epithelial cells, *Shigella* activates NF-κB via peptidoglycan sensing by the pattern recognition receptor Nod1,[6] thereby triggering the secretion of CXCL8. This event initiates the inflammatory cascade that is the hallmark of shigellosis in the colonic mucosa. These pathogens induce cell death in macrophages mainly through a 'NLCR4 inflammasome'- and caspase-1-mediated pyroptosis[7] accompanied by the subsequent release of IL-1β and IL-18 that exacerbates the severity of inflammation.[7,8] Others studies reported that *Shigella* is equally able to kill macrophages through necrosis, oncosis and a caspase-9-mediated apoptosis.[9–11] Furthermore, in fibroblasts *Shigella* infection provokes necrotic cell death through a pathway dependent on the host oxidative stress responses.[12] However, mechanisms of cell death tuning by *Shigella* are more complex than a simple induction of death. In fact, *Shigella*-infected HeLa cells can be partially protected from staurosporine (STP)-induced apoptosis,[13] or undergo to massive caspase-9-mediated apoptosis on lysis of these pathogens resident in host cell cytoplasm.[14]

Therefore, a picture emerges in which both inhibition and induction of different forms of cell death can coexist during cell infection by *Shigella*. The prevalent host cell response could be determined by the cell type, the multiplicity of infection (MOI), that is, the number of the invading bacteria, the

[1]Dipartimento di Biologia e Biotecnologie 'Charles Darwin', Sapienza-Università di Roma, Roma, Italy; [2]Dipartimento di Scienze Veterinarie,Università degli Studi di Camerino, Matelica (Macerata), Italy; [3]Dipartimento di Scienze Biomediche, Università degli Studi di Padova, Padova, Italy; [4]Dipartimento di Medicina Ambientale e Sanità Pubblica, Università degli Studi di Padova, Padova, Italy; [5]Department of Experimental Oncology European Institute of Oncology, Milan, Italy and [6]Istituto Pasteur-Fondazione Cenci Bolognetti, Sapienza-Università di Roma, Roma, Italy
*Corresponding author: ML Bernardini, Dipartimento di Biologia e Biotecnologie 'Charles Darwin', Istituto Pasteur-Fondazione Cenci Bolognetti, Sapienza-Università di Roma, Via Dei Sardi 70, Rome 00185, Italy. Tel: +39 6 49917850; Fax: +39 6 49917594; E-mail: marialina.bernardini@uniroma1.it
[7]Current Address: Institut Pasteur, Unité de Pathogénie Microbienne Moléculaire, 75724 Paris Cedex 15, France.
Keywords: apoptosis; mitochondria; *Shigella*; infection; Gadd45α
Abbreviations: MOI, multiplicity of infection; EVOC, *ex vivo* human organe culture; PCD, programmed cell death; GADD45α, growth arrest and DNA damage 45α; CHX, cycloheximide; TNF-α, tumor necrosis factor-α; STP, staurosporine; TMRM, tetramethylrhodamine methyl ester
Received 18.10.10; revised 28.12.10; accepted 10.1.11; Edited by RA Knight

presence of autocrine/paracrine effectors, the occurrence of stress reactions and by other not yet identified factors.

The purpose of this study is to further investigate on the host regulatory circuits that regulate the balance between death and survival in epithelial cells infected by *Shigella*. By using HeLa cells as an epithelial cell model system, we have analyzed: (i) the impact of the number of intracellular bacteria on the equilibrium of life/death; (ii) the type of cell death elicited by *Shigella* infection, focusing on the involvement of mitochondria and caspases in this process; and (iii) the pro- and anti-apoptotic transcriptome.

To assess whether the results obtained in HeLa cells mirror *in vivo* epithelial responses, we purposely developed a novel *ex vivo* model of *Shigella* infection of a human colonic mucosa. Finally, by exploiting these two experimental models, we identified the role of the stress sensor growth arrest and DNA damage 45α (Gadd45α) as a main host cell player in triggering the death of the cells infected by *Shigella*.

Results

HeLa cells infected with *Shigella* undergo a dose-dependent apoptosis. To examine the influence of the MOI on host cell death, we infected HeLa cells with *S. flexneri* wild-type strain M90T at MOI 10, 50 and 100 during a period of incubation (p.i.) of 5 h. The number of intracellular bacteria *per* cell increased rapidly at MOI 100, whereas it was significantly lower at MOI 10 and 50 (Figure 1a), as previously reported.[15]

Infected cells underwent apoptosis in a time- and MOI-dependent fashion, as shown by the number of both TUNEL- and annexin V-positive cells (Figures 1b and c and Supplementary Figure S1); especially, at 5 h p.i. 34% of the cells resulted positive to TUNEL analysis, while at this same time point, around 19 and 6% of the cells were positive at MOI of 50 and 10, respectively. These data strongly indicated that death of the infected cells is dependent on the number of intracellular bacteria. When HeLa cells were exposed to the noninvasive variant of M90T, BS176, we did not detect any apoptosis induction even after 12 h of infection (Supplementary Figures S2A and C), indicating that the death of HeLa cells was strictly dependent on the intracellular residence of bacteria.

Shigella infection triggered caspase-3 activation in a time- and MOI-dependent manner (Figure 2A) matching the kinetics and the degree of annexin-V positivity and cell death (compare Figures 2A and 1b; Supplementary Figure S1). At MOI of 100, starting from 3 h p.i. caspase-3 was significantly fourfold higher with respect to the control uninfected cells. At 5 h p.i., this value was of about 3.7-fold and 6-fold over the controls at MOI of 50 and 100, respectively (Figure 2A). The noninvasive strain BS176 did not elicit any caspase-3 activation at any time analyzed (Supplementary Figure S2B).

In order to assess the activity of apical caspases, we infected HeLa cells with wild-type strain M90T at a MOI 100. Both caspase-8 and caspase-9 were already activated at 1 h p.i. with a similar kinetics and degree (Figures 2B and C: compare with the positive controls STP and cycloheximide (CHX)/tumor necrosis factor (TNF)-α, respectively). Fluorescence studies performed by using the binding of fluorescent-coupled peptides inhibitors to the activated forms of caspase-9 (FLICA-caspase-9 (FAM-LEHD-FMK)) and caspase-8 (FLICA-caspase-8 (FAM-LETD-FMK)) confirmed that epithelial cells infected with M90T, transformed with DsRed plasmid vector, triggered the activation of both initiator caspases (Figures 2D and E).

To understand the relative role played by each of the two apical caspases in caspase-3 activation, previously determined by luminometric assay, we carried out a dual strategy. First, we assessed whether *Shigella* infection induced an early mitochondrial depolarization, which triggers caspase-9-mediated activation of caspase-3 in intrinsic apoptotic pathway. Other groups have already reported mitochondrial dysfunction on *Shigella* infection of fibroblasts.[12,16] Accordingly, by using flow cytometry analysis we found that about one-third of the infected cells displayed depolarized mitochondria as early as 1 h p.i. (Figures 3a and b). In addition, we observed that, starting from the first hour of infection, a fraction of cells undergoing mitochondrial membrane depolarization also displayed the caspase-3 activation, as assayed by the binding of the fluorescent-coupled DEVD inhibitor to the activated form of caspase-3 (FLICA caspase-3 (FAM-DEVD-FMK)). Second, we exploited an RNAi strategy in order to silence either caspase-8 or caspase-9. We observed that the caspase-3 activity was significantly reduced in the presence of RNAi for caspase-9, that is, 1.7 ± 0.19 *versus* 3.9 ± 0.05 at 3 h of incubation p.i. and 1.4 ± 0.3 *versus* 6 ± 0.19 following 5 h of incubation p.i. (Figure 3c). We did not observe any difference in caspase-3 values in the presence of RNAi for caspase-8 (Figure 3d), suggesting that an early caspase-8 activation is not necessary to induce apoptosis following *Shigella* infection, whereas the intrinsic apoptotic pathway is responsible for effector caspase activation.

Apoptotic and anti-apoptotic circuits activated during *Shigella* invasion. To understand the mechanisms of apoptosis regulation by *Shigella*, we analyzed the apoptosis transcriptome of HeLa cells infected with M90T at MOI 100 at 1, 3 and 5 h of incubation p.i.

We used an oligonucleotide array spotted with 135 apoptotic and anti-apoptotic genes (see Materials and methods section) and identified a panel of genes differentially expressed, which were subjected to hierarchical clustering to reveal expression trends (Figure 4a and Supplementary Table S1).

The expression profile was similar at the three time points examined with a small subset of genes differentially expressed under these three conditions of infection (see Supplementary Table S1). Hierarchical clustering identified three main categories of gene transcripts. The first group, which includes the majority of analyzed transcripts, was downregulated at the three time points with respect to the noninfected HeLa cells (e.g., *bik* or *bcl2*). In the second group, we classed the genes downregulated at 1 h and upregulated at 3 and 5 h (e.g., *jun or bclX_L*); finally, the third group encompasses the genes permanently activated with a sustained upregulation (e.g., *gadd45α* or *bad*).

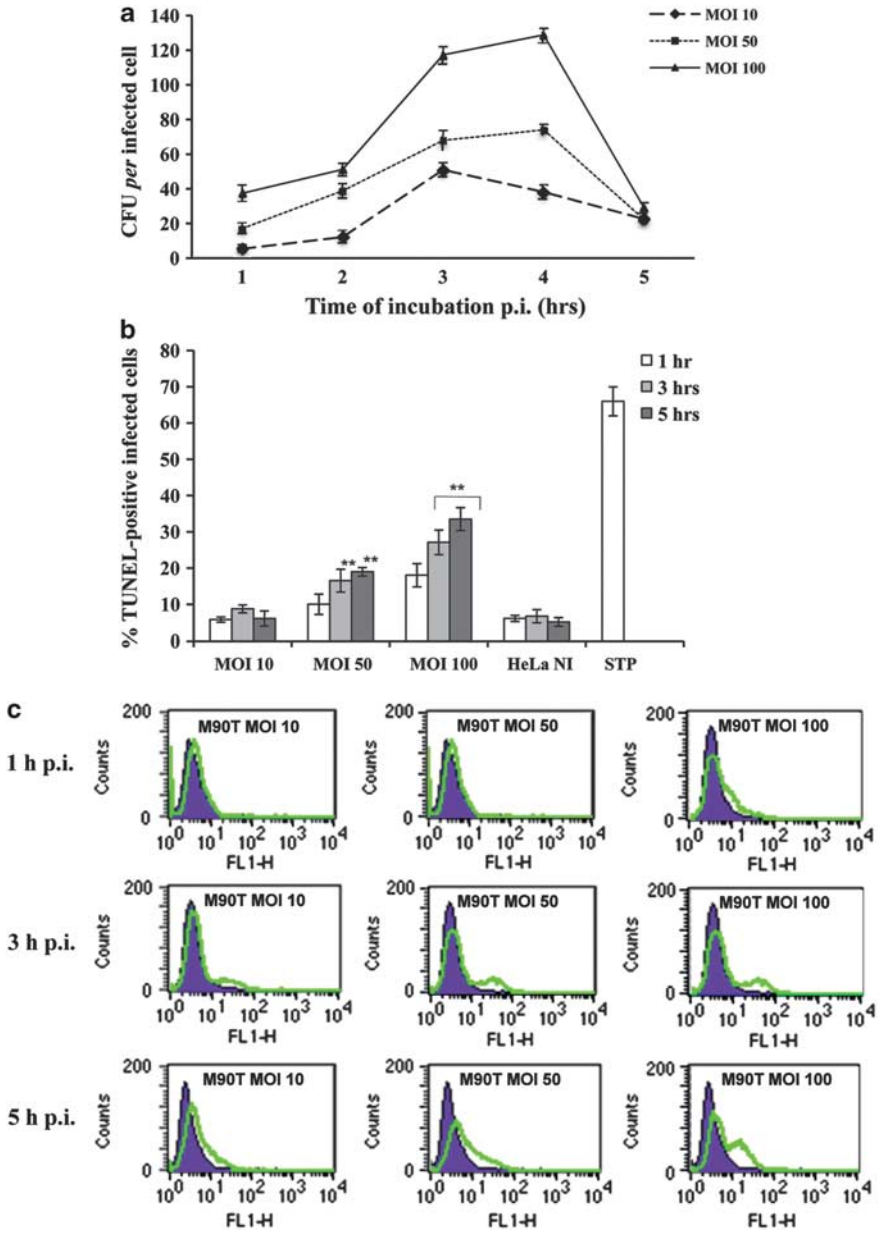

Figure 1 Intracellular growth kinetics of *S flexneri* M90T in HeLa cell monolayers and host cell death. (**a**) Kinetics of intracellular bacterial growth of the invasive *S. flexneri* strain M90T during 5 h of incubation p.i. at MOI 10, 50 and 100; (**b**) TUNEL assay on HeLa cells infected with *Shigella* as above. HeLa NI, non-infected HeLa cells; STP, non-infected HeLa cells treated for 4 h with STP (2 μM). (**c**) A representative cytofluorimetric output of TUNEL analysis performed at 1 h (upper panel), 3 h (middle panel) and 5 h of incubation p.i. (lower panel). Tunel-positive (i.e., dead) cells display an increased FITC staining (green line in the graph). In (**a** and **b**), bars represent the mean values ± S.D. from five independent experiments. $^{**}P < 0.01$ after Student's *t*-test

Down- or upregulation of a representative number of mRNAs was verified by quantitative real-time PCR (Figure 4b), confirming in the majority of cases the same trend of regulation shown by microarray analysis (e.g., *bad*, *bax*, *bcl2, bclX$_L$, nf-κb1, gadd45α*). However, the level of regulation of some of these transcripts, such as *akt2*, *bik*, *birc2* (*IAP-1*) and *birc3* (*IAP-2*) was deeply underestimated by the microarray study (compare Figure 4b and Supplementary Table S1). The modulation of Akt, IAP-1 and IAP-2 proteins could dramatically influence the balance between survival and apoptosis during *Shigella* infection, as all these proteins display a potent survival activity at different steps of the apoptotic cascade. Therefore, we verified whether the transcriptional upregulation of mRNA for Akt2, IAP-1 and IAP-2 was matched by a corresponding increase in their protein level. As reported in Figure 4c, we found that the Akt protein level strongly increased from 1 h p.i., while that of IAP-1/2 raised especially at 3 h p.i. We then assessed the modulation of anti- and pro-apoptotic proteins of the Bcl-2 family. We found a complex pattern of regulation (Figure 4d): induction of both pro-apoptotic (Bad) and anti-apoptotic (Bcl-X$_L$) proteins, but also repression of the

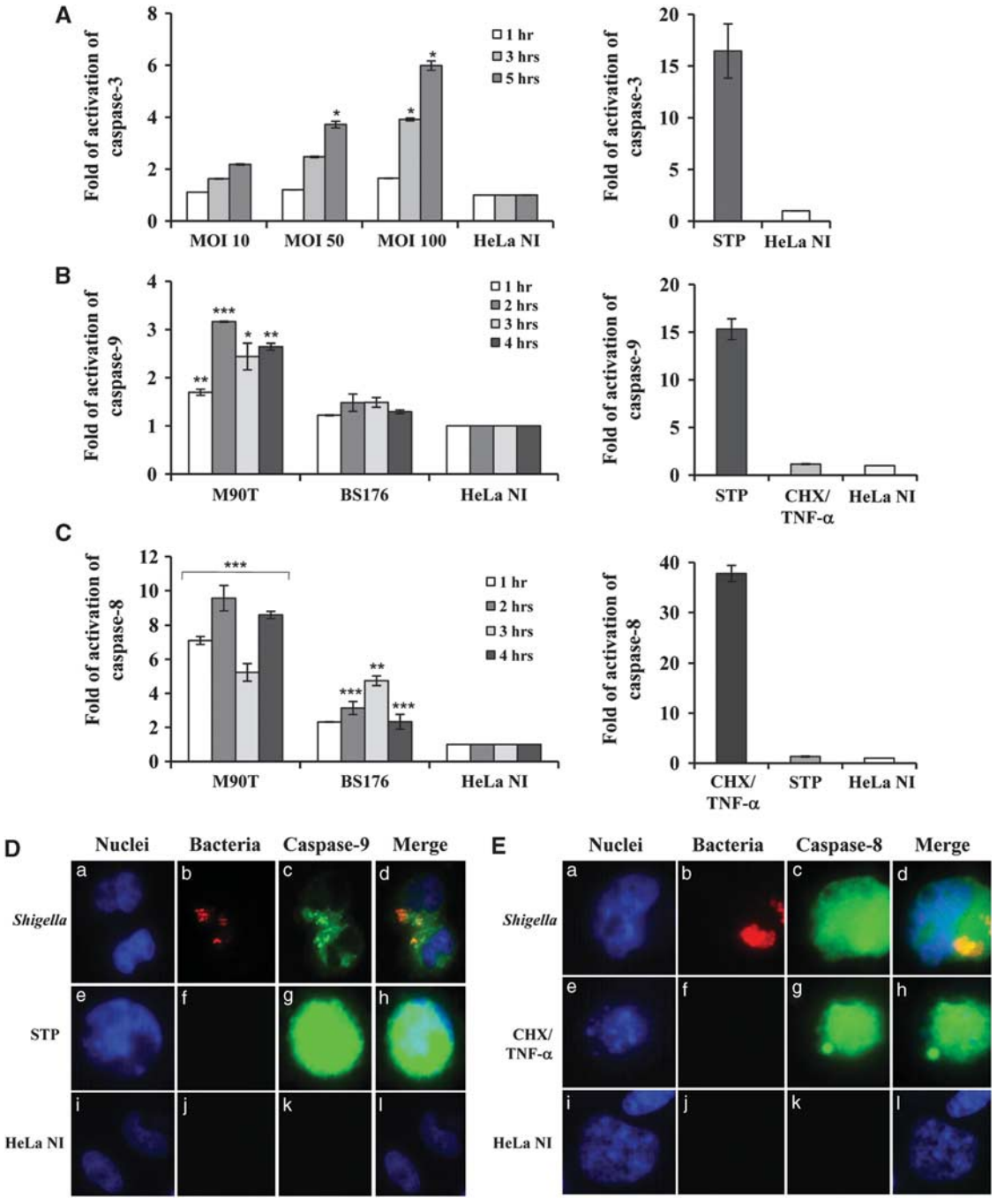

Figure 2 Caspase activation in HeLa cells infected with *Shigella*. (**A**) Kinetics of caspase-3 activation following infection of HeLa cells with M90T at different MOIs as above. (**B**) Caspase-9 and (**C**) caspase-8 activity in HeLa cells infected with M90T and its noninvasive variant BS176 (MOI of 100) at the reported time points. HeLa cells treated for 4 h with STP (2 μM) or with CHX (10 μg/ml) plus TNF-α (100 ng/ml) for 12 h were used as a control of caspase-9/3 and caspase-8 activation, respectively. HeLa NI, non-infected HeLa cells. Report assay data correspond to the mean ± S.D. (triplicate determinations) and are representative of three independent luminometric assays. $^{*}P<0.05$, $^{**}P<0.01$, $^{***}P<0.001$ after Student's *t*-test. (**D** and **E**) Immunofluorescence analysis of caspase-9 (**D**) and caspase-8 (**E**) maturation in HeLa cells infected with M90T-DsRed (MOI 100) at 2 h of incubation p.i. (a, b, c, d panels) Treated with STP or CHX plus TNF-α, as above (e, f, g, h panels in **D** and **E**, respectively) and uninfected (i, j, k, l panels). Cells were processed for labeling with fluorescent-coupled LEHD inhibitor to the activated form of caspase-9 (FLICA caspase-9 (FAM-LEHD-FMK)) or fluorescent-coupled LETD inhibitor to the activated form of caspase-8 (FLICA caspase-8 (FAM-LETD-FMK)) and DAPI. Shigellae, expressing DsRed plasmid vector, are stained in red. Magnification: × 40

death-inducing Bax and of the pro-survival Bcl-2. Altogether, these results suggest that modulation of the levels of Bcl-2 family members is not a primary event in apoptosis induction by *Shigella* infection. In accordance with both microarray and qPCR data, we found that the protein amount of Gadd45α, a protein describes as acting as a pro-apoptotic

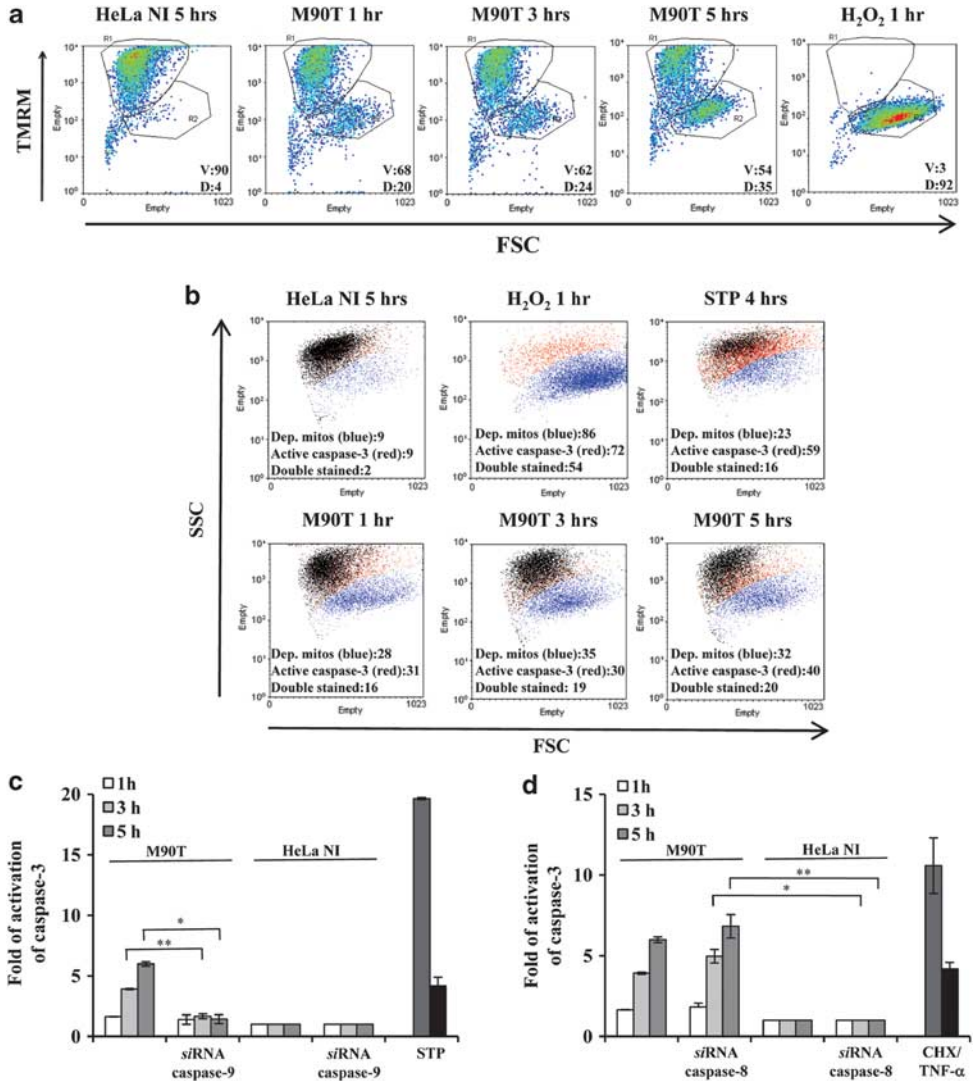

Figure 3 *Shigella*-infected HeLa cells undergo intrinsic apoptosis. (**a**) FACS analysis (forward scatter, FSC, *versus* TMRM) showing mitochondrial depolarization. The percentages of viable cells (V, TMRM positive, in the R1 quadrant) and of depolarized cells (D, TMRM negative, in the R2 quadrant) are reported. (**b**) FACS analysis of mitochondrial potential (TMRM staining; blue population) and of caspase-3 activation (FLICA caspase-3 labeling; red population). Both populations were determined on diagrams FSC *versus* fluorophore, and are shown together on a FSC *versus* SSC plot. In (**a** and **b**), HeLa cells were infected with M90T (MOI 100) for the reported time points; treatment with H_2O_2 (5 mM for 1 h) and with STP as in Figure 2 were used as positive controls of mitochondrial depolarization and of caspase activation. Cells transiently transfected with *si*RNA for caspase-9 (**c**) or for caspase-8 (**d**) were infected with M90T at MOI 100 and caspase-3 activity was measured at the reported time points. HeLa cells treated for 4 h with STP or with CHX plus TNF-α as specified in Figure 2 were used as a control. HeLa NI, non-infected HeLa cells. Report assay data correspond to the mean ± S.D. (triplicate determinations) and are representative of five independent luminometric assays. $^*P<0.05$, $^{**}P<0.01$, $^{***}P<0.001$ after Student's *t*-test

player,[17] was significantly upregulated during infection (Figure 4d).

Involvement of Gadd45α in *Shigella*-mediated cell death. *Gadd45α* is a stress-inducible gene regulated by a variety of genotoxic and non-genotoxic stresses. Gadd45α may have an important role as both a pro-apoptotic[17–19] and pro-survival factor as well.[20] Given the sustained upregulation of Gadd45α in infected HeLa cells, we asked whether and to which extent Gadd45α could be involved in *Shigella*-mediated apoptosis. We analyzed caspase-9, -8 and -3 activity and DNA fragmentation in HeLa cells depleted of Gadd45α through RNAi and infected with M90T as above. Uninfected cells or cells transfected with scramble *si*RNA and infected as above were used as controls. We found that caspase-9 maturation was dramatically abrogated in the presence of RNAi for Gadd45α, starting from 1 h of incubation p.i. (Figure 5B), while caspase-8 activity remained unaltered (Figure 5A).

In accordance with data of caspase-9 inhibition, HeLa cells expressing Gadd45α *si*RNA and infected with M90T displayed a strong decrease in caspase-3 activity (Figure 5C) and a significant reduction of DNA fragmentation (Figures 5E and F). We therefore investigated whether the lack of Gadd45α could affect caspase-3 activation following STP treatment that engages the intrinsic apoptotic pathway as *Shigella* does.

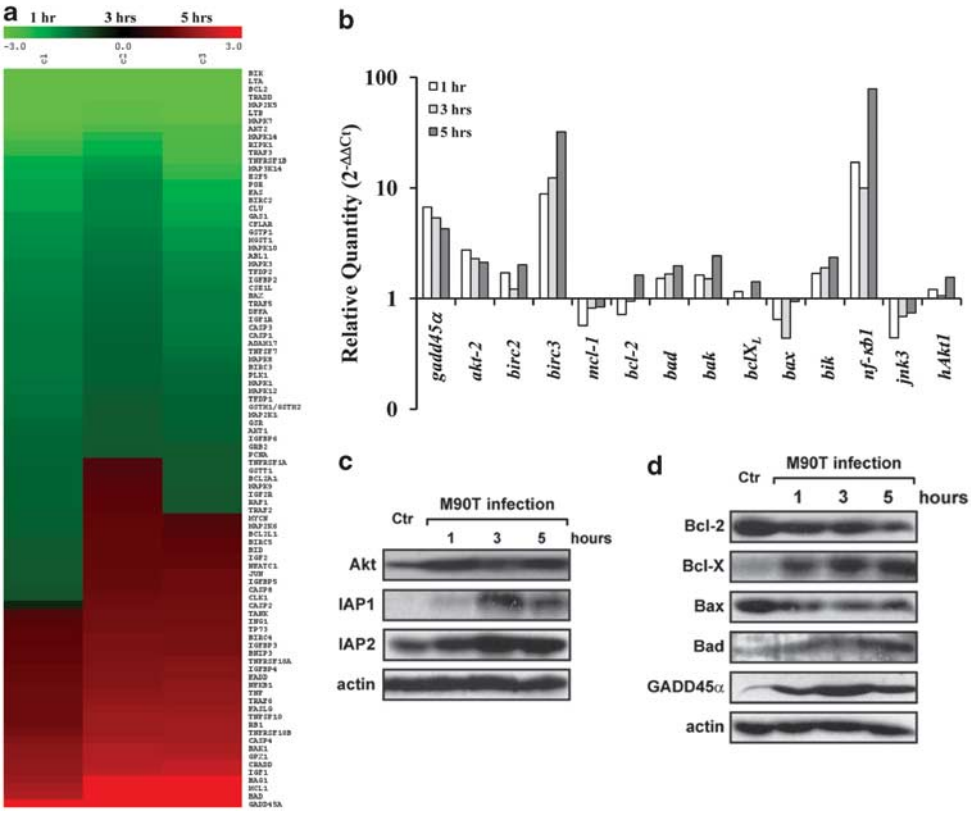

Figure 4 Modulation of pro- and anti-apoptotic gene expression in HeLa cells on infection with *S. flexneri* M90T. (**a**) Transcriptional profile of pro- and anti-apoptotic genes expressed by HeLa cells infected with *S. flexneri* M90T (MOI 100) at 1, 3 and 5 h of incubation p.i. Red and green colors represent up- and downregulation of gene expression, respectively, as compared with uninfected cells. The key for intensity of expression is indicated under the bar. (**b**) Validation/determination through qPCR for a representative subset of genes whose expression is highly modulated by *Shigella* infection. Results are normalized to the internal *gapdh* gene control and are presented on a logarithmic scale as the ratio of gene expression between infected and uninfected HeLa cells. (**c** and **d**) Western immunoblot analysis of changes in protein expression levels of HeLa cells following *Shigella* infection. Cell lysis was carried out at the reported time points. Blots were probed with actin as a loading control

As expected, Gadd45α-interfered HeLa cells treated with STP showed low level of caspase-3 values (Figure 5D) while no significant changes in caspase-3 activity was recorded in cells treated with CHX plus TNF-α, confirming that Gadd45α is mainly involved in the mitochondrial pathway of apoptosis.

***Shigella*-mediated epithelial cell apoptosis in an *ex vivo* human colon organ culture (EVOC) model of infection.** Not many animal systems have proven to be reliable models of *Shigella* infection. To overcome this limitation, we exploited here a recently developed technique allowing us to mimic as much as possible the human conditions. The three-dimensional architecture present in the EVOC guarantees the maintenance of physical parameters fundamental for several functions of the cells, such as spatial orientation and impact of gravity.

Therefore, human colonic specimens were apically infected with 10^8 CFU of M90T or BS176 and incubated overnight (ON). After this time, the samples were treated for histopathological and immunohistochemical (IH) analysis.

To determine the impact of *Shigella* on epithelial cell survival in the organotypic culture, we analyzed the morphological changes through hematoxylin/eosin (HE) staining. As shown in Figure 6B (panel a), the mucosa architecture of the uninfected samples remained unaltered and only scattered inflammatory cells were interspersed throughout the chorion.

In tissue sections infected with M90T, the epithelial layer was fully disorganized showing severe degeneration and death areas (Figure 6B, panel b). Indeed, an abundant inflammatory infiltrate organized in a pseudo-follicular structure was also evident. In contrast, tissues infected with BS176 did not display any significant alteration of the epithelium (Figure 6B, panel c).

Cells containing shigellae were highlighted by immunolabeling the bacterial lipopolysaccharyde (LPS). Intensity of LPS presence was scored as previously described[21] and reported in Figure 6A. As expected, no immunolabeling was noticed in uninfected sample (Figure 6B, panel d) while in the M90T-infected sections an intense intra- and extra-cellular immunostaining was present in the epithelial layer or free in mucus that covers the epithelium (Figure 6B, panel e). With BS176, LPS-immunostaining was mainly concentrated into the mucus, in accordance with the noninvasive phenotype of this strain (Figure 6B, panel f).

In serial sections of the colonic tissue, IH analysis of caspase-3 maturation evidenced that in uninfected colonic mucosa only rare positive cells (located in the epithelium and

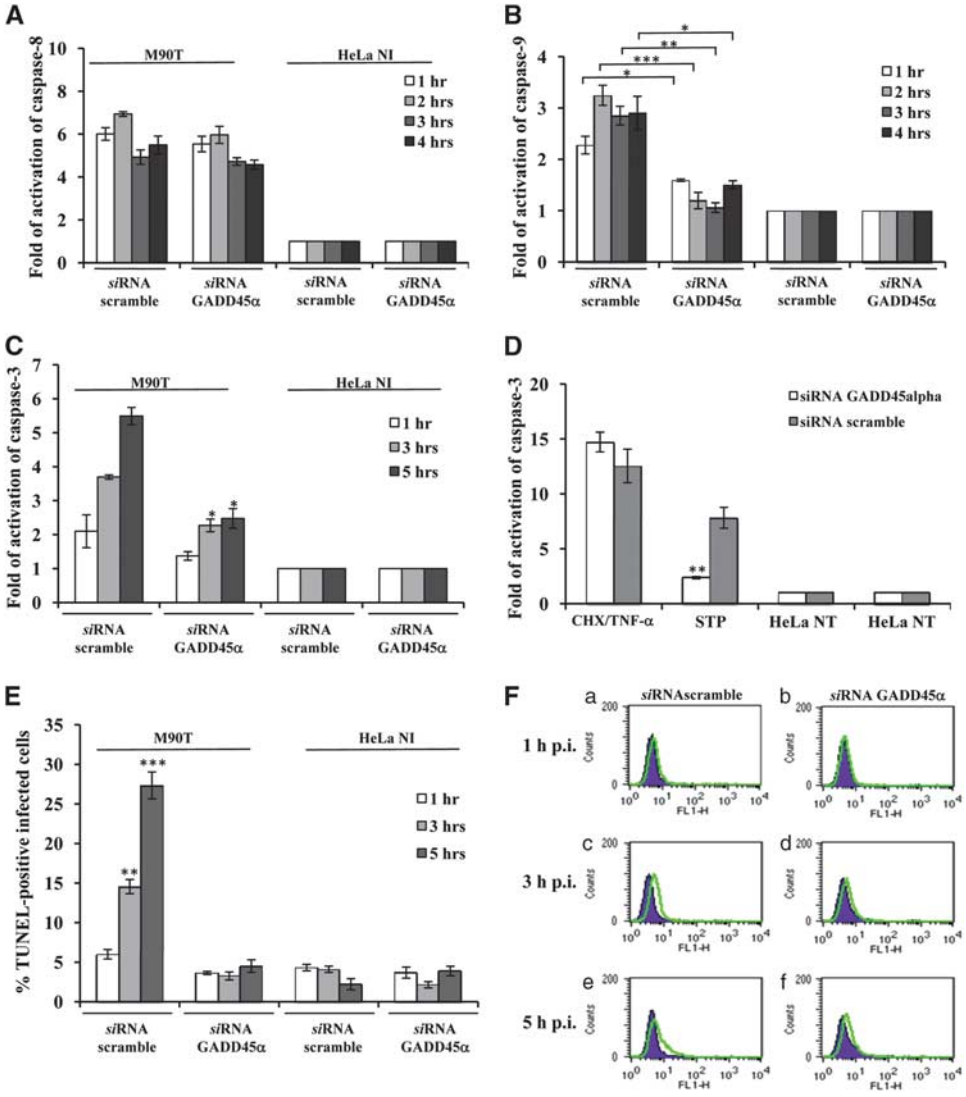

Figure 5 Gadd45α triggers *Shigella*-mediated apoptotic cell death in infected HeLa cells. Activity of caspase-8 (**A**), caspase-9 (**B**) and caspase-3 (**C**), and TUNEL assay (**E** and **F**) on HeLa cells transiently transfected with a Gadd45α or a scramble *si*RNA. Cells were infected with M90T at MOI of 100 for the reported time points. HeLa cells treated with STP or with CHX plus TNF-α, as detailed in Figure 2, were used as a control (**D**). HeLa NI, non-infected HeLa cells. Report assay data correspond to the mean ± S.D. (triplicate determinations) and are representative of three independent luminometric assays. $*P<0.05$, $**P<0.01$, $***P<0.001$ after Student's *t*-test. (**F**) A representative cytofluorimetric output of TUNEL analysis performed at 1 h (upper panel, a and b), 3 h (middle panel, c and d) and 5 h of incubation p.i. (lower panel, e and f)

chorion) were present (Figures 6A and B, panel g). With M90T, extensive areas of epithelial cells and some cells throughout the inflammatory infiltrate resulted marked by caspase-3 immunostaining (Figures 6A and B, panel h). Mucosa infected with BS176 showed a pattern of caspase-3 labeling similar to the uninfected cells (Figure 6B, panel i).

In the same histological sections, uninfected or infected by *Shigella*, the expression of Gadd45α was restricted mainly to the epithelial layer (Figure 6B, panels j, k, l). A strong immunostaining was evident in cells infected with M90T (Figures 6A and B, panel k), in which a colocalization of Gadd45α and LPS was also observed (data not shown). Moreover, Gadd45α immunolabeling retraced the distribution observed with caspase-3 staining (compare panels h with k). Notably, Gadd45α upregulation was not found in mesenchimal or in mononuclear cells (i.e., lympho-monocytes or plasma cells) of mucosal chorion; this observation is in accordance with the analysis performed by different authors in lungs where Gadd45α expression is restricted to the airway epithelium and type II pneumocytes, also in the presence of phlogosis characterized by inflammatory infiltrate or BALT activation.[22]

Finally, a constant colocalization of Gadd45α, cleaved caspase-3 and TUNEL nuclear-positive reaction was observed in stained serial sections of M90T-infected tissues (Figure 6B, panels h, k and n).

In contrast to these observations, control (Figure 6B, panel m) and BS176-infected samples (panel o) showed mild surface disarray, scarce colonocyte apoptosis and relative preservation of surface and crypt architecture, associated

with rare co-expression of Gadd45α and a TUNEL-positive reaction.

We may conclude that the use of this novel polarized *ex vivo* organ culture system highlights that *Shigella*-induced epithelial cell apoptosis is associated with Gadd45α upregulation.

Discussion

In this study, we demonstrate that *Shigella* invasion of epithelial cells: (i) regulates the expression of a complex pool of pro- and anti-apoptotic genes; (ii) induces a rapid apoptosis, mainly via caspase-9 activation and mitochondrial

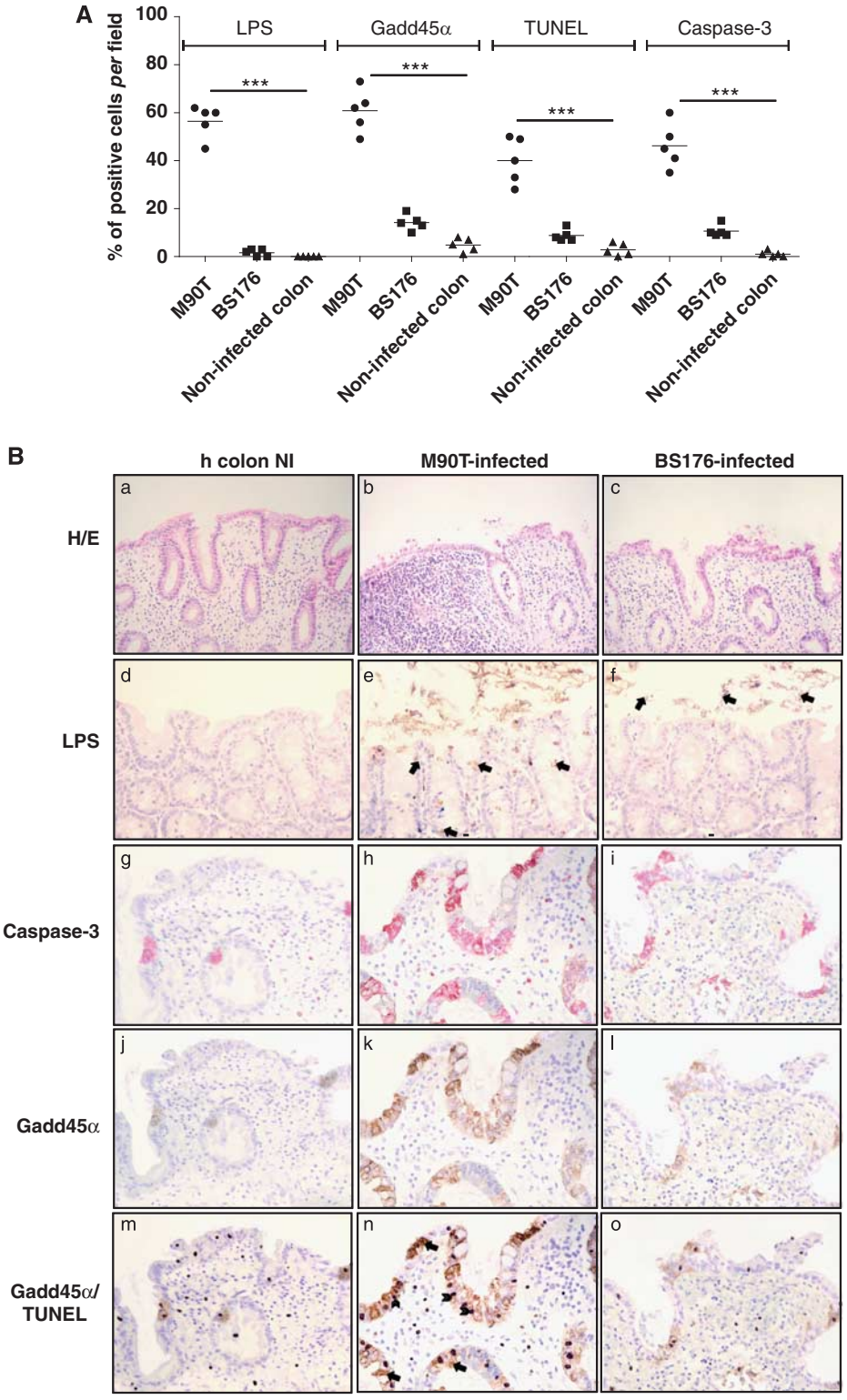

involvement; and (iii) activates the pro-apoptotic factor Gadd45α, which in turn has a key role in the execution of the apoptotic process.

Different groups have tackled the issue of death regulation on *Shigella* infection of non-myeloid cells. Results have often been puzzling, as both cell death induction (either apoptotic or necrotic) or inhibition have been reported.[12,13] These diverse observations reflect the complexity of host cell responses to *Shigella* invasion. In this view, changes of experimental parameters such as target cell type (MEF *versus* HeLa cells), MOI, time of infection (from 1 to 24 h), effective number of intracellular bacteria and the use of exogenous adhesion systems (e.g., AFA E, *E. coli* afimbrial adhesin), could well account for the heterogeneity of reported results.

Indeed, our results are in agreement with this complexity of responses, as we observe regulation of both pro- and anti-apoptotic proteins. Several pathogens, including *Legionella* and *Chlamydia*, induce the expression of pro-survival genes to maximize their persistence in host cells.[23] We found that infection with *Shigella* elicits the expression of several potent pro-survival factors, such as c-IAP-1, c-IAP-2, Akt and Bcl-X_L. Both IAP proteins and Akt interfere through a variety of mechanisms with apoptotic pathways[24,25] and were reported to be upregulated or activated on *Shigella* infection.[26,27] In the case of Bcl-X_L, its anti-apoptotic activity is balanced on the mitochondrial surface by multiple interactions with both anti- and pro-apoptotic Bcl-2 family members.[28] We observed a complex response endowed with inhibition of the pro-survival Bcl-2 and of the apoptogenic Bax, and with induction of Bad, another pro-apoptotic family member. Thus, we can envision a scenario characterized by the simultaneous activation of apoptotic and anti-apoptotic pathways, whose balance is finely modulated during infection with *Shigella* toward the eventual commitment to death of the infected cell.

As for the type of cell death prompted by *Shigella* invasion, both Dupont *et al.*[16] and Carneiro *et al.*[12] report ROS production and mitochondrial membrane depolarization following a 5–8-h infection at MOI 100 of MEFs. Both groups conclude that *Shigella* causes necrotic cell death in the MEF model. Our results agree with these observations, in that we have observed both ROS production (data not shown) and mitochondrial depolarization in infected HeLa cells, and these events are detectable as early as 1 h p.i. at MOI 50 (see Figures 3a and b). However, it must be highlighted that, even if mitochondrial membrane depolarization constitutes a point of no return in cell death induction, accounting for ROS production and respiratory arrest, release of Ca^{2+}, pyridine nucleotides and of a pool of apoptogenic proteins,[29] it can be upstream to either necrosis or apoptosis, depending on a wide set of variables, such as the bioenergetic status of the cell,[30–32] the intensity of the noxious stimulus or the availability of a functioning apoptotic machinery.[33] When apoptosis occurs downstream to mitochondrial depolarization, this is specifically hallmarked by activation of caspases.

In line with this issue, we demonstrate activation of both initiator and effector caspases, TUNEL positivity and phosphatidylserine exposure on the host cell surface. We also show caspase-3 activation and TUNEL positivity in epithelial cells infected with *Shigella* in EVOC model, emphasizing the importance of apoptosis induction following infection of epithelial cells.

Notably, during *Shigella* infection, a fraction of HeLa cells undergoing mitochondrial depolarization also displays caspase activation (double stained cells in Figure 3b), demonstrating that mitochondrial damage occurs in apoptotic cells. Another fraction of cells is endowed with mitochondrial depolarization, but without any detectable caspase activity (the blue population in Figure 3b). These could be either cells entering the apoptotic process, upstream to caspase induction or necrotic cells, in accord with Dupont and Carneiro. It is possible that at a higher MOI, the proportion of necrotic cells could increase even in our experimental model, as stress conditions might be too intense for the set-up of the apoptotic response (e.g., a massive mitochondrial depolarization could cause a rapid ATP depletion, making caspase activation impossible).

In accordance with a mitochondrial involvement in apoptosis induction, activation of the key effector caspase-3 is almost abolished by knocking-down caspase-9 (Figure 3c) but not caspase-8 (Figure 3d), despite its early activation at 1 h p.i. (Figure 2C). Notably, caspase-8 is also transiently induced by the noninvasive strain, which is unable to cause cell death. Altogether these observations indicate that caspase-8 is rapidly activated by *Shigella*, possibly through interactions with membrane death receptors; but this activation is not required for a full-blown apoptotic process, which instead relies on a secondary induction of the intrinsic caspase-9-dependent pathway downstream to mitochondrial depolarization.

Furthermore, we found that induction of Gadd45α is a main effector event in apoptosis triggering by *Shigella*. In fact, *gadd45α* is strongly and rapidly induced in HeLa cells and its depletion dramatically reduces *Shigella*-induced apoptosis. Both caspase-9/3 activation (Figures 5B and C) and TUNEL positivity are abrogated by Gadd45α knock-down, whereas caspase-8 induction is not affected, indicating that the intrinsic branch of apoptosis induction is specifically affected by the Gadd45α absence. Consistently, in EVOC model *gadd45α* is strongly induced in cells displaying caspase-3 activation and TUNEL positivity (Figures 6A and B) although this activation

Figure 6 Apoptosis assessment and Gadd45α expression in a human *ex vivo* organ culture (EVOC) invasion assay with *S. flexneri* M90T. (**A**) Dot blot of the distribution of LPS, Gadd45α, TUNEL and caspase-3 immunostained epithelial cells in sections of human colon biopsies infected with M90T or BS176 (12 h) or uninfected. Immunohistochemically stained cells were counted at × 400 magnification. For each sample, five view fields in five sections were considered for cell enumeration. Circles represent the mean values *per* sample while the horizontal line represents the mean value *per* sample category. ***$P<0.001$ after Student's *t*-test. (**B**) Histopathological and IH characterization of human colon sections infected with M90T or BS176 or uninfected. Upper panels (HE and LPS): HE (a, b, c) HE staining; LPS (d, e, f): IH staining of *S. flexneri* 5 LPS, in e and f bacterial LPS are indicated by arrows. In HE original magnification 200; in LPS original magnification × 400. Lower panels: analysis in serial sections of EVOC of immunolabeled mature caspase-3 (g, h, i), Gadd45α (j, k, l) and colocalization of Gadd45α immunostaining and positive TUNEL nuclei, Gadd45α/TUNEL (m, n, o). All relevant informations are reported in the figure. Arrowheads indicate TUNEL-positive cells and arrows indicate cell positively immunostained by the Gadd45α mAb. In caspase-3, Gadd45α and Gadd45α/TUNEL panels, original magnification × 400. Human colon NI: uninfected human colon; M90T-infected: EVOC infected over-night with 10^8 CFU of M90T; BS176-infected: EVOC infected over-night with 10^8 CFU of BS176

does not involve a parallel modulation of p53 (data not shown).

Gadd45α is known to be upregulated in response to a variety of cell stresses in order to elicit cell cycle arrest at the G2-M transition and to regulate the apoptotic response.[17–19] Several studies highlight the pro-apoptotic role of Gadd45α in different type of cells such as breast cancer cells, keratinocytes and HeLa.[34,35] The mode of apoptosis induction by Gadd45α is still debated, and could involve activation of the p38/JNK signaling pathways[34] and/or activation of pro-apoptotic Bcl-2 family proteins.[18] Consistently with this issue, we found that the pro-apoptotic Bcl2 family member Bad is upregulated and over-produced during *Shigella* infection. Moreover, the pro-survival pathway governed by the MAPKs could be impaired by the decreased expression of the genes encoding these proteins during infection. However, Gadd45α protects from apoptosis hematopoietic cells exposed to genotoxic stress.[34] In the framework of bacterial infection, it has been reported that challenge of oral epithelial cells with the invasive opportunistic pathogen *Fusobacterium nucleatum* induces Gadd45α expression, while the noninvasive oral commensal *Streptococcus gordonii* does not.[36] Consequently, these investigators propose that Gadd45α could act as a stress sensor following bacterial invasion of epithelial cells, even if a mechanistic proof is still lacking.

Conclusively, we demonstrate for the first time that activation of Gadd45α following bacterial invasion of epithelial cells is required for the building-up of the apoptotic response through activation of its intrinsic branch, which is the one responsible for *Shigella*-mediated cell death. Furthermore, the observation that Gadd45α is activated in the colonic epithelial cells opens new perspectives in the study of factors influencing the outcome of pathogenesis of shigellosis.

Materials and Methods

Bacterial strains, plasmids and growth conditions. The *S. flexneri* 5a strains used are M90T streptomycin-resistant (Sm^R) and its noninvasive derivative BS176 (ref. 21). *S. flexneri* M90T-DsRed strain was created by transforming wild-type strain with DsRed plasmid vector (gently gifted by Maria Rescigno). The presence of DsRed plasmid vector did affect neither T3SS function, as demonstrated through effector proteins comassie blue staining or *Shigella* invasiveness, tested by the HeLa cell infection assay (data not shown). In addition to this, DsRed plasmid has no toxic effect on eukaryotic cells, as already reported.[37] Bacteria were grown in Trypticase soy broth (BBL, Becton Dickinson and Co., Cockeysville, MD, USA) or agar (TSA). Streptomycin (Sm) and ampicillin (Ap) were added to cultures at 100 μg/ml.

Cell culture and infections. HeLa cells were maintained in D-MEM supplemented with 10% FBS (both by Cambrex BioScience, Walkersville, MD, USA). HeLa cell infections with invasive and noninvasive strains were performed as previously reported[15] using the MOI of 10, 50 and 100. Incubation of cells and bacteria in the presence of gentamicin (60 μg/ml) was prolonged to 1, 2, 3, 4 or 5 h, depending on the experiment. At desired time points of incubation, infected HeLa cells were processed to evaluate parameters associated with apoptosis. Intracellular multiplication of bacteria in HeLa cells was assayed as described previously.[15]

Cell death studies, caspases activity and annexin V staining. Apoptosis was assessed using TUNEL fluorometric (DeadEnd TUNEL fluorometric system, Promega, Milano, Italia) and annexin V staining (Annexin V-FITC Apoptosis Detection kit, BD Pharmingen, San José, CA, USA), according to the manufacturer's instructions. Both TUNEL and annexin V binding were analyzed using a flow cytometric analysis on a FACSCalibur cytometer (Becton Dickinson, San Josè, CA, USA). Data acquisition (10^4 events for each sample) was performed using CellQuest software (Becton Dickinson, San Jose, CA, USA). Uninfected cells and cells treated for 4 h with 2 μM STP, (Sigma Aldrich, Milano, Italia) were used in parallel. Cells deemed TUNEL or FITC-annexin V positive were those displaying fluorescence greater than the fluorescence of non-infected HeLa cells (control).

At desired time point of incubation post infection (p.i.), the activities of caspase-3, -8 and -9 were determined through a luminometric system by using Caspase Glo kit (Promega). Uninfected cells and cells treated for 4 h with 2 μM STP or alternatively for 12 h with CHX (10 μg/ml) (Sigma-Aldrich) plus TNF-α, (100 ng/ml) (R&D System, Minneapolis, MN, USA), were used as controls. Results are reported as fold induction of relative luciferase units over unstimulated cells. Relative luciferase activity is calculated as the ratio between the absolute caspase luminescent values normalized to cell vitality (Cell titer Glo, Promega). Data are expressed as the mean ± S.D. of at least five experiments performed in triplicate.

***si*RNA assays.** *si*RNA inhibition of caspase-8, caspase-9 and Gadd45α was carried out by using HP validated *si*RNA, all purchased from Qiagen (Milano, Italia): Hs_CASP8_11_HP validated *si*RNA (NM_001228), Hs_CASP9_7_HP validated *si*RNA (NM_001229) and Hs_ Gadd45α_5_HP validated *si*RNA (NM_001924), respectively. Caspase-8 and caspase-9 depletion was verified by western blot analysis with purified mouse anti-human caspase-8 monoclonal antibody (clone 3-1-9, BD Pharmingen, San José, CA, USA) and monoclonal anti-human caspase-9 (clone LAP6, R&D System), respectively. A monoclonal anti-β-tubulin (clone TUB 2.1, Sigma-Aldrich) antibody was used as a control. Gadd45α depletion was evaluated through RT-PCR (Supplementary Information Figure S3).

HeLa cells were transfected with 5 nM double-stranded *si*RNA using HiPerfect transfection reagent (Qiagen) according to the manufacturer's protocol. For caspase-8 and caspase-9 at 96 h after transfection, cells were infected in order to evaluate caspase-3 activity, as detailed above. Otherwise, for Gadd45α caspases' activity and TUNEL analysis were carried out in HeLa cells infected following 48 h from transfection.

Analysis of mitochondrial membrane potential. Evaluation of mitochondrial membrane potential ($\Delta\psi_M$) was carried out by flow cytometric analysis by staining infected and uninfected HeLa cells with mitochondrion-selective probe tetramethylrhodamine methyl ester (TMRM), as already reported.[38] Uninfected cells treated for 45 min with H_2O_2 (Sigma-Aldrich) at the concentration of 5 mM, were the positive control. Briefly, infected cells were detached from dishes, washed once in phosphate-buffered saline (PBS) and re-suspended in 50 μl HEPES buffer (10 mM HEPES, 135 mM NaCl, 5 mM $CaCl_2$). Samples were incubated for 15 min at 37 °C in TMRM (200 nM), freshly prepared from stock solution 10 mM in DMSO. Value acquisition was carried out on a FACSCalibur cytometer, as reported above; analysis was performed with WinMDI software (WinMDi, Joseph Trotter, The Scripps Institute, Flow Cytometry Core Facility). Evaluation of apoptotic (caspase-3/TMRM)-infected HeLa cells was carried out by flow cytometric analysis by double staining infected and uninfected HeLa cells with TMRM and caspase-3, as above.

Immunofluorescence of caspase-8 and -9 activities. Caspase-8 and caspase-9 maturation were also evaluated through fluorescence microscopy staining by using Carboxyfluorescein FLICA Apoptosis Detection kit Caspase assay (Immunochemistry Technologies, LLC, Bloomington, MN USA). Staining protocol was set up according to the manufacturer's instructions. At specified time points, infected HeLa monolayers were washed once in PBS, fixed for 10 min in 3,7% paraformaldheyde solution and incubated for 1 h at 37 °C under 5% CO_2 in 1X FLICA solution, freshly prepared from stock solution 30X in DMSO. Nuclei were stained for 3 min with 2 μg/ml 4′-6-diamidino-2-phenylindole (DAPI) solution. Uninfected cells and cells treated for 4 h with 2 μM STP or alternatively for 12 h with CHX plus TNF-α, as above, were used as controls.

Stained cells were examined using a Leica DMRE microscope and images were recorded on Leica DC250 camera and processed using Qwin software (Leica Microsystems, Milano, Italia).

Microarray and real-time PCR. Expression level of pro- and anti-apoptotic genes in *S. flexneri*-infected HeLa monolayers was evaluated by using Dual Chip microarrays Human apoptosis kit (Eppendorf, Milano, Italia) as recommended by the manufacturer. Uninfected cells or HeLa cells infected at MOI 100 were processed after 1, 3 and 5 h of incubation p.i. and total RNA was extracted by using RNeasy Plus Mini Kit (Qiagen). Approximately, 5 μg of total RNA was used for biotin-dNTP cDNA synthesis and labeling, by using Superscript II Reverse

Transcriptase (Invitrogen, Milano, Italia). Biotinylated cDNA was labeled by using Silverquant Detection Kit (Eppendorf), as recommended by the instructions. Hybridization protocol and washing steps were performed according to the manufacturer's suggestions. Image data acquisition and gene expression profiling analysis were carried out by applying Silverquant analysis software (Eppendorf) (Supplementary Information Table S1).

Quantitative real-time PCR (qPCR) and western blot analysis were applied to validate gene expression profiling. For qPCR 10 ng of cDNA, from both uninfected and M90T-infected HeLa cells, was used in each reaction. qPCR was carried out in triplicate by using Power SYBR Green PCR Master Mix (Applied Biosystem, Monza, Italia), in 30 μl reaction volume, by using a 7300 Real-Time PCR System (Applied Biosystem). The $2^{-\Delta\Delta Ct}$ method was applied to analyze the relative changes in expression profiling of interest genes, as already reported.[39] Values were normalized to the internal *gapdh* gene control. Primers for qPCR were designed through Primer Express software (Applied Biosystem) and are listed in Supplementary Information File S1.

Western blot. Total cell extracts were prepared at 4 °C in 135 mM NaCl, 20 mM Tris-HCl pH 7.5, 1 mM $CaCl_2$, 1% Triton X-100 in the presence of phosphatase and protease inhibitors. Samples were then separated in reducing conditions on SDS-polyacrylamide gels and transferred onto Hybond-C Extra membranes (Amersham, Little Chalfont, UK). Primary antibodies were incubated 16 h at 4 °C, and horseradish peroxidase-conjugated secondary antibodies were added for 1 h. Proteins were visualized by enhanced chemiluminescence (Amersham). The goat polyclonal anti-actin antibody, the rabbit polyclonal anti-IAP1, anti- IAP2, anti-Bax, anti-Bad, anti-Gadd45α antibodies were from Santa Cruz Biotechnology (Santa Cruz, CA, USA); the mouse monoclonal anti-Bcl-2 antibody was from Becton Dickinson Pharmingen (Franklin Lakes, NJ, USA); the rabbit monoclonal anti-Bcl-X_L and the rabbit polyclonal anti-Akt antibodies were from Cell Signaling (Beverly, MA, USA).

EVOC model of infection. All patients are informed on admission that tissue samples or organs obtained during diagnostic or treatment procedures may be also used for research purposes, through an appropriate informed consent form approved by the Ethics Committee of the European Institute of Oncology (IEO).

The assay was performed in accordance to a protocol recently developed by Ktisilingiri *et al.* (submitted). Briefly, healthy colonic tissues were obtained from patients undergoing surgery for colon cancer. Collected tissue samples, maintained in Hank's balanced salt solution, were transported to the laboratory and processed within the next hours. Mucosa layer, separated from the underlying tissues, was then divided in pieces of about 1 cm^2 and oriented mucosal surface upward on sterile metal grids. Cylinder was attached to the tissue on the top of the mucosa layer with the use of surgical glue. Then, the samples were put on to a center-well tissue culture petri dishes containing 1 ml of medium. 100 μl of bacterial logarithmic growth culture (approximately 1×10^8 bacteria) were added inside the cylinder and the petri dishes were incubated in 95% O_2–5% CO_2 atmosphere inside an airtight container at 37 °C for 12 h. Following incubation, colonic-infected tissues were fixed in 4% paraformaldeyde and processed for histological and IH analyses. As a routinely procedure, EVOC tissue sections were first immunostained with an anti-Ki-67 mAb, which is a marker for cell proliferation. Only samples showing a positive reaction for the presence of this protein were processed for further histopathological and IH studies.

Immunohistological studies. Samples for histological and IH analysis were fixed in 10% buffered formalin and paraffin embedded. Three-micrometer-thick sections were stained with HE stain for histopathological examination. For IH tests, sections were treated as previously reported.[21] Briefly, to localize *S. flexneri* antigen in infected tissues and to characterize immunohistochemically the apoptosis and related molecules in epithelial/inflammatory cell populations the following antibodies were used on serial sections: rabbit polyclonal anti-*Shigella flexneri* 5a LPS, rabbit pAb anti-Gadd45α (1 : 50, Millipore Corporate Headquarters, Billerica, MA, USA), rabbit pAb anti-cleaved caspase-3 (1 : 10, anti-active caspase-3 pAb, Promega Corporation). In particular, expression of cleaved caspase-3 was investigated using an affinity-purified rabbit polyclonal antibody directed against a peptide from the p18 fragment of the cleaved human caspase-3 and evaluated as suggested by Resendes *et al.*[40] Antibody-binding was revealed through ABC-peroxydase or ABC – alkaline phosphatase techniques using 1 : 200 diluted biotin conjugated goat-anti rabbit immunoglobulin G (Vector Laboratories, Inc., Burlingame, CA, USA) and a 1 : 200 diluted biotinylated goat-anti mouse Ig (AO433; DAKO, Glostrup, Denmark), applied for 45 min at room temperature as secondary antibodies. The enzymatic reaction was developed with 3-1-diaminobenzydine (DAB, with/without nichel) (Sigma Chemical Co., St. Louis, MO, USA) or VIP (Vector) as substrates. For all antibodies used, the primary antibody was replaced by PBS as a negative control.

In colonic sections apoptotic index in epithelial and inflammatory cells was highlighted through a TUNEL colorimetric staining (DeadEnd, Promega) according to the manufacturer's instructions.

To score the consistence of Gadd45α, caspase-3 and TUNEL-positive cells in M90T- and BS176-infected and uninfected samples, five random fields of the sample were examined under a dry-X40 objective. The number of epithelial-positive cells was normalized to the number of epithelial cells *per* field.

Statisticals. Data were presented as mean ± S.D., and the numbers of independent experiments were indicated in each legend of the figures. Statistical calculations and tests were performed using the Student's *t*-test. A *P*-value < 0.05 was considered statistically significant. A *P*-value < 0.001 was considered extremely significant.

Conflict of Interest

The authors declare no conflict of interest.

Acknowledgements. This work was partially supported by grants from the Italian 'Ministero dell'Istruzione, Università e Ricerca' (PRIN 2009). Luigi Lembo-Fazio, Giulia Nigro and Gaëlle Noël were fellows of the 'Istituto Pasteur-Fondazione Cenci Bolognetti'. Katerina Tsilingiri is a recipient of a Marie-Curie fellowship within the cross-talk network.

1. Labbe K, Saleh M. Cell death in the host response to infection. *Cell Death Differ* 2008; **15**: 1339–1349.
2. Deretic V, Levine B. Autophagy, immunity, and microbial adaptations. *Cell Host Microbe* 2009; **5**: 527–549.
3. Mathan VI, Mathan MM. Intestinal manifestations of invasive diarrheas and their diagnosis. *Rev Infect Dis* 1991; **13** (Suppl 4): S311–S313.
4. Sansonetti PJ, Ryter A, Clerc P, Maurelli AT, Mounier J. Multiplication of *Shigella flexneri* within HeLa cells: lysis of the phagocytic vacuole and plasmid-mediated contact hemolysis. *Infect Immun* 1996; **51**: 461–469.
5. Parsot C. *Shigella flexneri*: genetics of entry and intercellular dissemination in epithelial cells. *Curr Top Microbiol Immunol* 1994; **192**: 217–241.
6. Girardin SE, Boneca IG, Carneiro LA, Antignac A, Jehanno M, Viala J *et al.* Nod1 detects a unique muropeptide from gram-negative bacterial peptidoglycan. *Science* 2003; **300**: 1584–1587.
7. Suzuki T, Franchi L, Toma C, Ashida H, Ogawa M, Yoshikawa Y *et al.* Differential regulation of caspase-1 activation, pyroptosis, and autophagy via Ipaf and ASC in *Shigella*-infected macrophages. *PLoS Pathog* 2007; **3**: e111.
8. Hilbi H, Chen Y, Thirumalai K, Zychlinsky A. The interleukin 1beta-converting enzyme, caspase 1, is activated during *Shigella flexneri*-induced apoptosis in human monocyte-derived macrophages. *Infect Immun* 1997; **65**: 5165–5170.
9. Koterski JF, Nahvi M, Venkatesan MM, Haimovich B. Virulent *Shigella flexneri* causes damage to mitochondria and triggers necrosis in infected human monocyte-derived macrophages. *Infect Immun* 2005; **73**: 504–513.
10. Nonaka T, Kuwae A, Sasakawa C, Imajoh-Ohmi S. *Shigella flexneri* YSH6000 induces two types of cell death, apoptosis and oncosis, in the differentiated human monoblastic cell line U937. *FEMS Microbiol Lett* 1999; **174**: 89–95.
11. Suzuki T, Nakanishi K, Tsutsui H, Iwai H, Akira S, Inohara N *et al.* A novel caspase-1/toll-like receptor 4-independent pathway of cell death induced by cytosolic *Shigella* in infected macrophages. *J Biol Chem* 2005; **280**: 14042–14050.
12. Carneiro LA, Travassos LH, Soares F, Tattoli I, Magalhaes JG, Bozza MT *et al. Shigella* induces mitochondrial dysfunction and cell death in nonmyleoid cells. *Cell Host Microbe* 2009; **5**: 123–136.
13. Faherty CS, Maurelli AT. Spa15 of *Shigella flexneri* is secreted through the type III secretion system and prevents staurosporine-induced apoptosis. *Infect Immun* 2009; **77**: 5281–5290.
14. Tattoli I, Lembo-Fazio L, Nigro G, Carneiro LA, Ferraro E, Rossi G *et al.* Intracellular bacteriolysis triggers a massive apoptotic cell death in *Shigella*-infected epithelial cells. *Microbes Infect* 2008; **10**: 1114–1123.
15. Cersini A, Salvia AM, Bernardini ML. Intracellular multiplication and virulence of *Shigella flexneri* auxotrophic mutants. *Infect Immun* 1998; **66**: 549–557.
16. Dupont N, Lacas-Gervais S, Bertout J, Paz I, Freche B, Van Nhieu GT *et al. Shigella* phagocytic vacuolar membrane remnants participate in the cellular response to pathogen invasion and are regulated by autophagy. *Cell Host Microbe* 2009; **6**: 137–149.

17. Gao M, Guo N, Huang C, Song L. Diverse roles of GADD45alpha in stress signaling. *Curr Protein Pept Sci* 2009; **10**: 388–394.
18. Tong T, Ji J, Jin S, Li X, Fan W, Song Y *et al.* Gadd45α expression induces Bim dissociation from the cytoskeleton and translocation to mitochondria. *Mol Cell Biol* 2005; **25**: 4488–4500.
19. Li Y, Qian H, Li X, Wang H, Yu J, Liu Y *et al.* Adenoviral-mediated gene transfer of Gadd45α results in suppression by inducing apoptosis and cell cycle arrest in pancreatic cancer cell. *J Gene Med* 2009; **11**: 3–13.
20. Zerbini LF, Wang Y, Czibere A, Correa RG, Cho JY, Ijiri K *et al.* NF-kappa B-mediated repression of growth arrest- and DNA-damage-inducible proteins 45alpha and gamma is essential for cancer cell survival. *Proc Natl Acad Sci USA* 2004; **101**: 13618–13623.
21. Martino MC, Rossi G, Martini I, Tattoli I, Chiavolini D, Phalipon A *et al.* Mucosal lymphoid infiltrate dominates colonic pathological changes in murine experimental shigellosis. *J Infect Dis* 2005; **192**: 136–148.
22. O'Reilly MA, Staversky RJ, Watkins RH, Maniscalco WM, Keng PC. p53-independent induction of GADD45 and GADD153 in mouse lungs exposed to hyperoxia. *Am J Physiol Lung Cell Mol Physiol* 2003; **278**: L552–L559.
23. Rudel T, Kepp O, Kozjak-Pavlovic V. Interactions between bacterial pathogens and mitochondrial cell death pathways. *Nat Rev Microbiol* 2010; **8**: 693–705.
24. Srinivasula SM, Ashwell JD. IAPs: what's in a name? *Mol Cell* 2008; **30**: 123–135.
25. Downward J. PI 3-kinase, Akt and cell survival. *Semin Cell Dev Biol* 2004; **15**: 177–182.
26. Pedron T, Thibault C, Sansonetti PJ. The invasive phenotype of *Shigella flexneri* directs a distinct gene expression pattern in the human intestinal epithelial cell line Caco-2. *J Biol Chem* 2003; **278**: 33878–33886.
27. Pendaries C, Tronchere H, Arbibe L, Mounier J, Gozani O, Cantley L *et al.* PtdIns5P activates the host cell PI3-kinase/Akt pathway during *Shigella flexneri* infection. *Embo J* 2006; **25**: 1024–1034.
28. Chipuk JE, Moldoveanu T, Llambi F, Parsons MJ, Green DR. The BCL-2 family reunion. *Mol Cell* 2010; **37**: 299–310.
29. Rasola A, Sciacovelli M, Pantic B, Bernardi P. Signal transduction to the permeability transition pore. *FEBS Lett* 2010; **584**: 1989–1996.
30. Gramaglia D, Gentile A, Battaglia M, Ranzato L, Petronilli V, Fassetta M *et al.* Apoptosis to necrosis switching downstream of apoptosome formation requires inhibition of both glycolysis and oxidative phosphorylation in a BCL-X(L)- and PKB/AKT-independent fashion. *Cell Death Differ* 2004; **11**: 342–353.
31. Nicotera P, Melino G. Regulation of the apoptosis-necrosis switch. *Oncogene* 2004; **23**: 2757–2765.
32. Orrenius S, Zhivotovsky B, Nicotera P. Regulation of cell death: the calcium-apoptosis link. *Nat Rev Mol Cell Biol* 2003; **4**: 552–565.
33. Rasola A, Bernardi P. The mitochondrial permeability transition pore and its involvement in cell death and in disease pathogenesis. *Apoptosis* 2007; **12**: 815–833.
34. Rosemary Siafakas A, Richardson DR. Growth arrest and DNA damage-45 alpha (GADD45alpha). *Int J Biochem Cell Biol* 2009; **41**: 986–989.
35. Hoffman B, Liebermann DA. Gadd45 modulation of intrinsic and extrinsic stress responses in myeloid cells. *J Cell Physiol* 2009; **218**: 26–31.
36. Hasegawa Y, Mans JJ, Mao S, Lopez MC, Baker HV, Handfield M *et al.* Gingival epithelial cell transcriptional responses to commensal and opportunistic oral microbial species. *Infect Immun* 2007; **75**: 2540–2547.
37. Martinoli C, Chiavelli A, Rescigno M. Entry route of *Salmonella typhimurium* directs the type of induced immune response. *Immunity* 2007; **27**: 975–984.
38. Rasola A, Geuna M. A flow cytometry assay simultaneously detects independent apoptotic parameters. *Cytometry* 2001; **45**: 151–157.
39. Livak KJ, Schmittgen TD. Analysis of relative gene expression data using real-time quantitative PCR and the 2(-Delta Delta C(T)). *Methods* 2001; **25**: 402–408.
40. Resendes AR, Majo N, Segales J, Espadamala J, Mateu E, Chianini F *et al.* Apoptosis in normal lymphoid organs from healthy normal, conventional pigs at different ages detected by TUNEL and cleaved caspase-3 immunohistochemistry in paraffin-embedded tissues. *Vet Immunol Immunopathol* 2004; **99**: 203–213.

Supplementary Information accompanies the paper on Cell Death and Disease website (http://www.nature.com/cddis)

Supplementary Information Figure S1. Annexin V/PI staining of M90T-infected epithelial cells. HeLa cells were infected with M90T at MOI 10, 50 and 100 and processed to evaluate apoptotic cell death through Annexin V/PI staining.

A representative histogram of FACS analysis performed at 1, 3 and 5 h p.i. is shown. Uninfected cells (HeLa NI) and uninfected HeLa cells treated with STP for 4 h were used as a control.

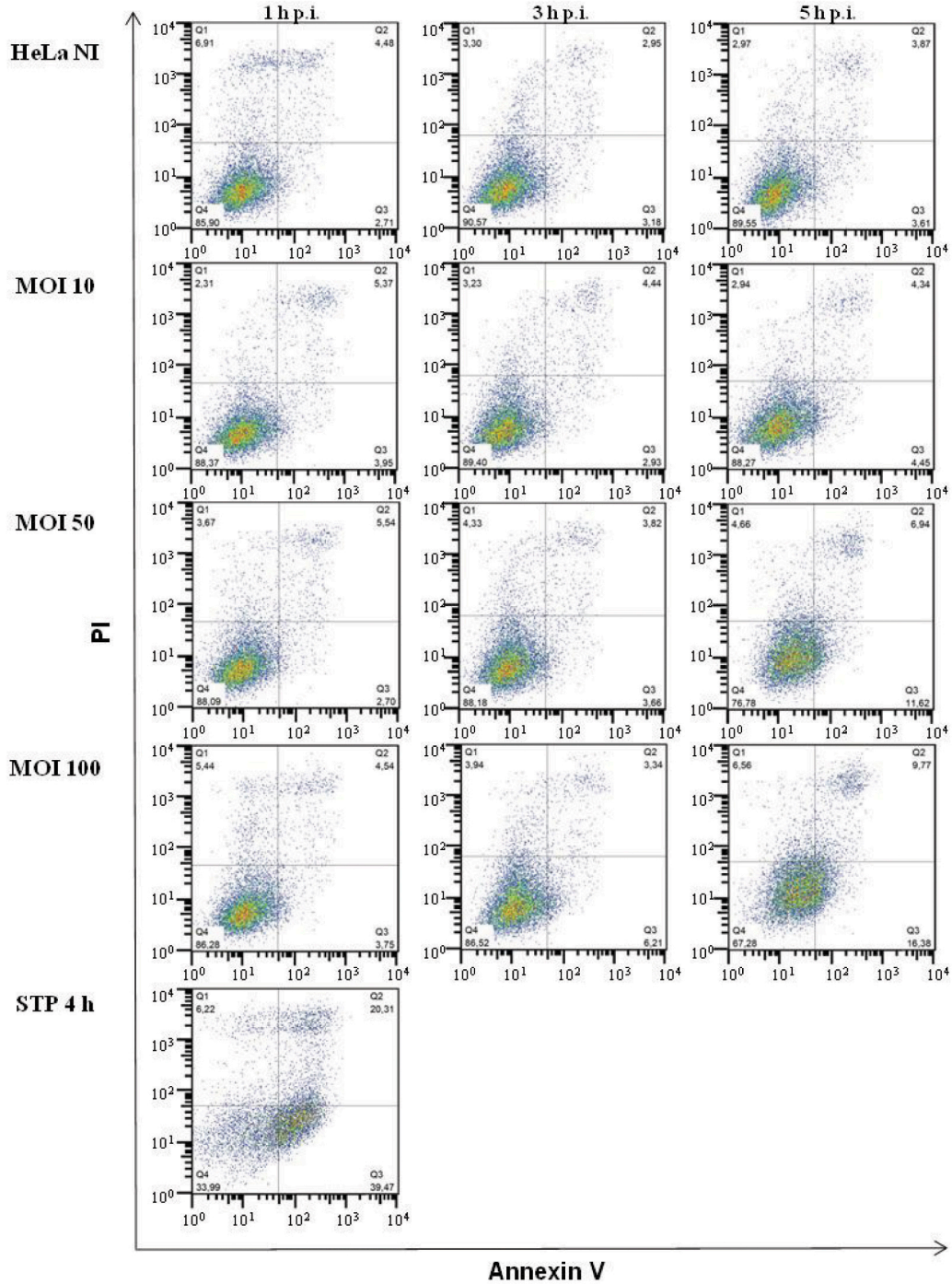

Supplementary Information Figure S2 Cell death analysis of epithelial cells infected with BS176. HeLa cells were infected with BS176 at MOI of 100 bacteria and processed to evaluate apoptotic process through TUNEL assay (**A**) capase-3 activity (**B**) and PI staining (**C**).

(**A**) A representative histogram of FACS analysis performed at 1h (a), 3 h (b) and 5 h p.i. (c) is shown. Uninfected cells were used as control. (**B**) HeLa cells were infected as above and processed following 1 h, 3 h and 5 h p.i. to evaluate caspase-3 activity through a luminometric assay. Uninfected cells (HeLa NI) and uninfected HeLa cells treated with CHX plus TNF-α for 12 h were used as control. Bars represent the mean values ± S.D. from 3 independent experiments. (**C**) A representative histogram of FACS analysis performed following 12 h p.i. is shown. Uninfected cells were used as control

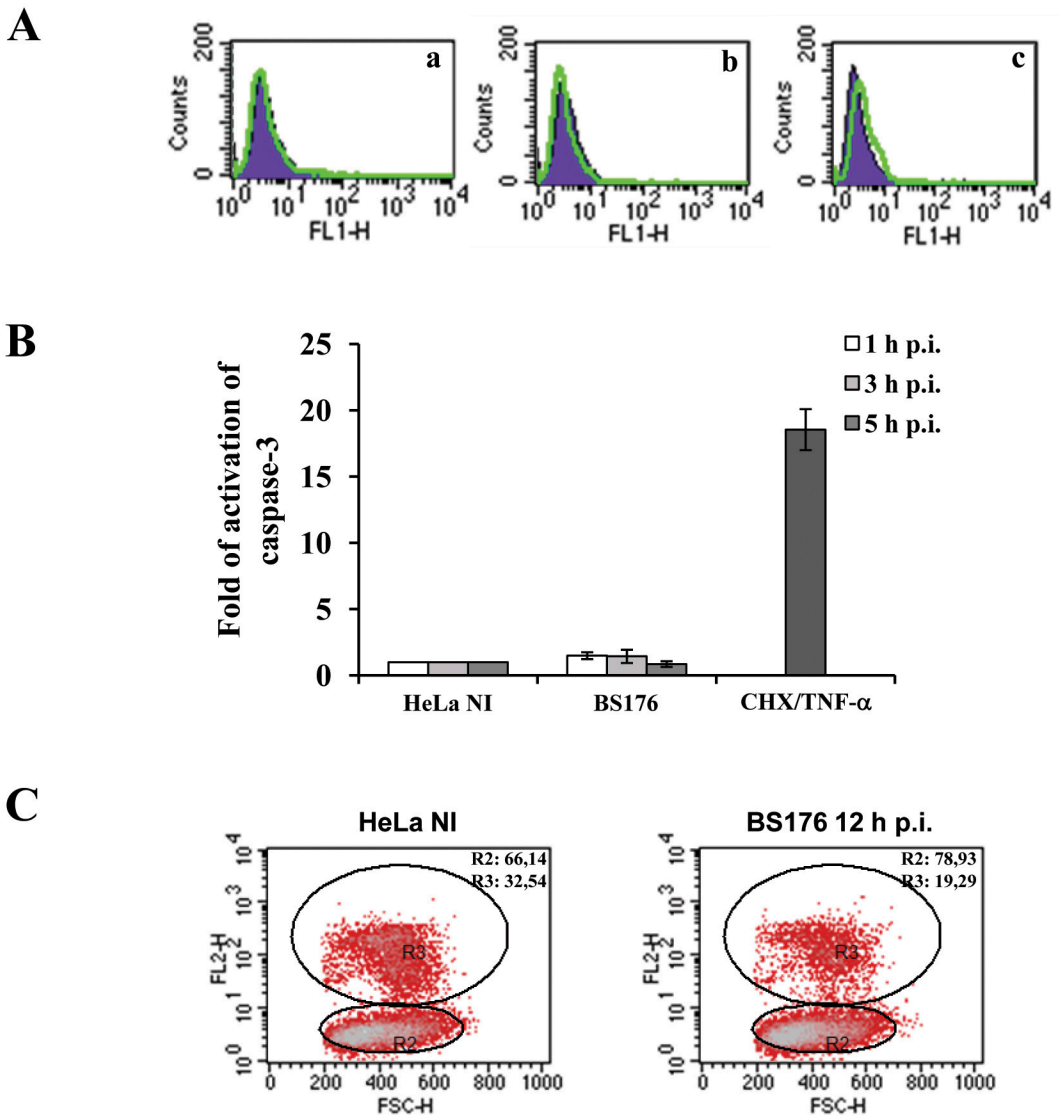

Supplementary Information Figure S3. Gadd45α mRNA expression analysis. HeLa cells, transiently transfected with *si*RNAGadd45α or alternatively with scramble RNA (siRNA scramble) were infected with M90T at MOI of 100 and processed, following 5 h p.i. in order to verify Gadd45α silencing through RT-PCR. Uninfected Gadd45α interfered HeLa cells or siRNA scramble uninfected HeLa cells were used as controls. Values were normalized to the internal *β-actin* gene control (bottom panel).

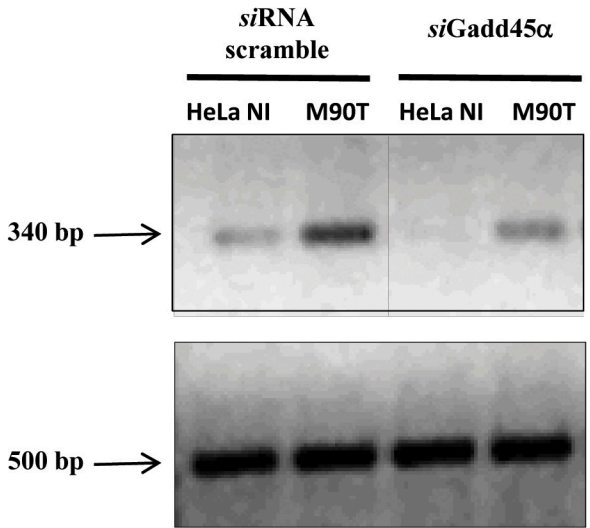

Supplementary Information File S1

Gene Name	Accession Number	Primer Sequences
akt1	NM_005163.1	*5' TCTATGGCGCTGAGATTGTG 3'* *5' CTTAATGTGCCCGTCCTTGT 3'*
akt2	NM_001626.2	*5' TGAAAACCTTCTGTGGGACC 3'* *5' TGGTCCTGGTTGTAGAAGGG 3'*
bad	NM_004322.2	*5' CGAGTGAGCAGGAAGACTCCA 3'* *5' AGAGTCCACAAACTCGTCACT 3'*
bak	U16811.1	*5' TCAACCGACGCTATGACT 3'* *5' TCTTCGTACCACAAACTGG 3'*
bax	NM_004324.1	*5' TGGAGCTGCAGAGGATGATTG 3'* *5' CCAGTTGAAGTTGCCGTCAGA 3'*
bcl2	NM_000633.1	*5' AGGAAGTGAACATTTCGGTGAC 3'* *5' GCTCAGTTCCAGGACCAGGC 3'*
bclX$_L$	NM_001191.1	*5' ATCATTTCCCCCCACTCTCC 3'* *5' TATCCCAAGCAGGCTGAATCC 3'*
bik	NM_001197.3	*5' CGCCAGAGGAGAAATGTCTGAA 3'* *5' ATGCCAAGAACCTCCATGGTC 3'*
birc2	NM_001166.3	*5' GTCAGAACACCGGAGGCATTT 3'* *5' ATTCGAGCTGCATGTGTCTGC 3'*
birc3	AF070674.1	*5' GCCATTGACTTTTCTGTCGCC 3'* *5' TTGCTCAATTTTCCACCACAGG 3'*
gadd45α	NM_001924.2	*5' GCCTGTGAGTGAGTGCAGAA 3'* *5' ATCTCTGTCGTCGTCCTCGT 3'*
gadph	NM_002046.2	*5' GACATCAAGAAGGTGGTGAAGC 3'* *5' TCTACCACCCTGTTGCTGTAG 3'*
mapk10 (jnk3)	NM_002753.2	*5' AACCAGTTCCTACAGTGTGGAAGTG 3'* *5' CTGAATCACTTGACATAAGTTGGC 3'*
mcl-1	AF118124.1	*5' GATGATCCATGTTTTCAGCGAC 3'* *5' CTCCACAAACCCATCCCAG 3'*
nf-κb1	NM_003998.1	*5' CCGTTATGTATGTGAAGG 3'* *5' AGAGTCCAGGATTATAGC 3'*